Journal of Hydroscience and Hydraulic Engineering
Vol. 18, No.2 November, 2000, 105-122

SWARMS OF FINE PARTICLES FALLING IN QUIESCENT AND FLOWING WATERS

By

Juichiro Akiyama, Masaru Ura, Hideki Nishimori and Naoki Yamashita

Department of Civil Engineering, Kyushu Institute of Technology
Tobata Kitakyushu 804-8550, Japan

SYNOPSIS

Motion of the particle cloud, that produced by direct dumping of a mass of fine particles, falling through quiescent and flowing fresh waters are investigated experimentally. A series of laboratory experiments is conducted, changing the size and the amount of dumped particles as well as the magnitude of ambient flow velocity. The transitional conditions from the thermal-like phase to the free settling-like phase are roughly estimated. Based on the homogeneous thermal theory, such major flow characteristics as half-width, mean buoyancy force and falling velocity of the particle clouds in quiescent and flowing waters are quantified as a function of the initial conditions, particle size and ambient flow velocity. Several important flow characteristics, including entrainment coefficient, shape factors, trajectory and others are also quantified.

INTRODUCTION

Direct dumping of soil by a bottom door-type hopper barge is able to reclaim economically coastal waters, and dredged material is disposed of in designated area of lakes and coastal waters. In such cases, a mass of dumped solid material often causes large scale pollution due to turbidity. In order to assess the environmental impact on fishes, benthic organisms and others at some distance from reclamation site, detailed information on hydrodynamics of a mass of particles falling in water is required.

Considerable number of studies have been devoted to understand and predict the hydrodynamics of the particle clouds falling in water. For instance, Tamai et al.(1) attempted to clarify the short-term fate of solid material dumped in quiescent ambient water. They found experimentally that the motion of a mass of falling particles takes both of the thermal-like and free-settling-like form, depending on the size of particles and the amount of dumped particles. They also proposed a theoretical model, that can describe the motion of a two-dimensional falling mass of particles changing its form from the thermal-like phase to the free-settling-like phase, by extending the homogeneous turbulent thermal theory developed by Baines and Hopfinger(2). Akiyama et al.(3) developed a two-dimensional homogeneous thermal theory that

includes drag force exerting on the cloud, and quantified the entrainment coefficient, drag coefficient and others. Buhler and Papantoniou(4) conducted a theoretical and experimental study on swarms of coarse particles. They found that, in the final stage of the particle cloud, the front velocity remains constant and somewhat larger than the terminal settling velocity of individual particles. Horie(5) developed a numerical model based on the MAC method and conducted numerical experiments to clarify the short-term fate of dumped solid material. Such approach is further pursued by Oda et al.(6) , Li(7) and Ying et al.(8). Oda et al.(6) developed a numerical model, based on the DEMAC, which consists of the DEM(9) and the MAC method, and investigated the effects of a mass of dumped particles on dispersion as well as settling of particles and the deposit profile. Li(7) studied particle clouds experimentally and numerically, and found that the velocity of the cloud approaches the terminal settling velocity of the individual particles and the growth rate of half-width of the cloud decreases with the settling velocity of particles. Ying et al.(8) developed a one-fluid numerical model based on the LES with the modified Smagorinsky model, and verified its validity by comparing with the experimental results for the falling as well as horizontal spreading stage formed after its impingement on the bottom. It is also found from numerical calculation that the added mass coefficient, employed in the thermal theory (3), is actually only one-half of that of a solid elliptic cylinder obtained by potential flow theory.

All of the studies cited above are concerned with the hydrodynamics of the dense or particle clouds in quiescent ambient water. However, as demonstrated numerically by Oda et al.(10) and experimentally by Akiyama et al.(11), presence of ambient flow somewhat affects to dynamics of the buoyant clouds. Oda et al.(10) applied the numerical model based on the DEMAC to a mass of particles falling through the flowing ambient water with logarithmic velocity profile, and found from numerical experiments that the shape, falling speed and width of the particle cloud, the deposit profile, and the induced motion of ambient flow are significantly influenced by the magnitude of ambient flow velocity, and that the cloud advects horizontally at about the same velocity as ambient flow velocity. Akiyama et al.(11) investigated experimentally the motion of a homogeneous dense cloud falling in a uniform ambient water, and confirmed Oda et al.'s finding that the cloud advects horizontally at almost the same velocity as ambient flow(10). It was also found that the falling velocity of the cloud follows the same relationship as the case of quiescent ambient water, but the entrainment coefficient becomes smaller than that in quiescent ambient water.

In this study, the motion of the particle cloud, that produced by direct dumping of a mass of fine particles, falling through quiescent and flowing fresh water are investigated experimentally. When the velocity of ambient water is larger than a certain magnitude, the cloud will be diffused. Such a situation is not the focus of this study. A series of laboratory experiments is conducted, changing the size and the amount of dumped particles as well as the magnitude of ambient flow velocity. The transitional condition from the thermal-like phase to the free settling-like phase is roughly estimated. Based on the homogeneous thermal theory(3) and the similarity collapse method(12), such major flow characteristics as half-width, mean buoyancy force and falling velocity of the particle clouds in quiescent and flowing water are quantified. Several important flow characteristics, including entarainment coefficient, shape factors, trajectory and others, also are quantified.

Table 1 Experimental condition

case	Median Diameter of Particle d(cm)	Submerged Specific Gravity of Particle s	Ambient Flow Velocity U(cm/s)	Initial Half-Volume per Unit Width A_o(cm^2)	Initial Total Buoyancy Per Unit Width W_o(cm^3/s^2)
1-a-1	0.0044	1.467	0	0.97	1394
1-a-2				1.94	2789
1-a-3				2.91	4183
1-a-4				3.88	5578
2-a-1	0.0088	1.480	0	1.04	1513
2-a-2				2.09	3026
2-a-3				3.13	4539
2-a-4				4.17	6052
3-a-1	0.0140	1.650	0	1.09	1757
3-a-2				2.17	3514
3-b-1			3.22	0.54	878
3-b-2				1.09	1757
3-b-3				1.63	2635
3-b-4				2.17	3514
3-c-1			6.22	1.09	1757
3-c-2				1.63	2635
3-c-3				2.17	3514
3-d-1			9.19	1.09	1757
3-d-2				1.63	2635
3-d-3				2.17	3514
4-a-1	0.0270	1.650	0	1.14	1845
4-a-2				2.28	3690
4-b-1			3.05	0.57	923
4-b-2				1.14	1845
4-b-3				1.71	2768
4-b-4				2.28	3690
4-c-1			6.11	0.29	469
4-c-2				0.57	923
4-c-3				0.86	1390
4-c-4				1.14	1845
4-d-1			8.88	0.57	923
4-d-2				0.86	1390
4-d-3				1.14	1845

EXPERIMENT AND DEFINITION

A particle cloud was generated by directly dumping fine particles (median diameter d, density ρ_p, specific gravity σ, free settling velocity of a particle V_f) with the initial total buoyancy $2W_o(=2sgA_o)$ from water surface into a body of fresh water with constant density ρ_a, where s is the

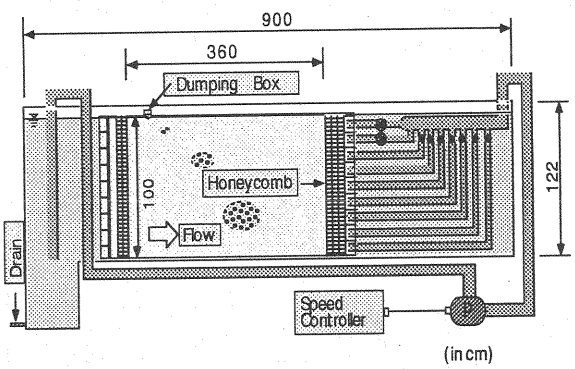

Fig.1 Experimental set-up (flowing ambient water)

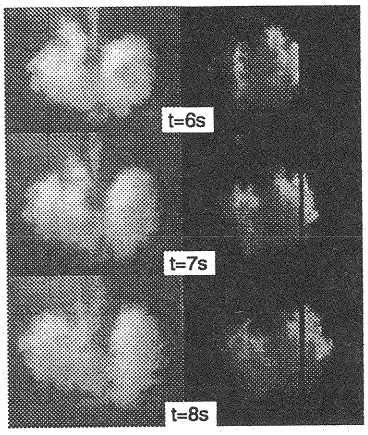

Fig.2 Motion of particle cloud (a:quiescent ambient water,b:flowing ambient water)

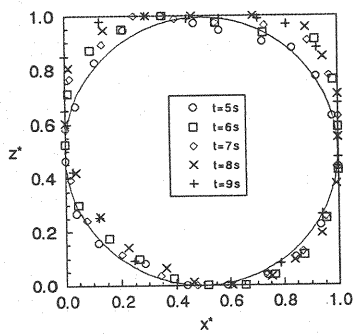

(a)

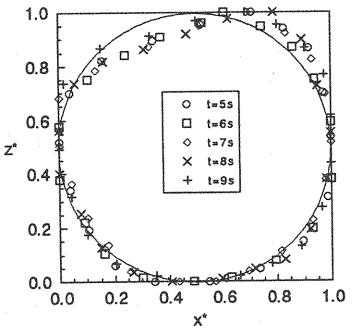

(b)

Fig.3 Comparison between similarity cloud shape and ellipse under different initial condition (a:quiescent ambient water,b:flowing ambient water)

submerged specific gravity of particle(= σ-1), A_0 the half-volume of particles per unit width, and g the acceleration due to gravity.

Two different experimental set-ups were used; a plexiglas tank (0.1m wide,1.5m deep, and 1.5m long) for the cases of quiescent ambient water and a plexiglas channel(0.1m wide, 1.00m deep, and 4.0m long) immerced in a water reservoir(0.6m wide, 1.22m deep , and 9.0m long) for the case of flowing ambient water, respectively. Uniform ambient water was generated in the immerced plexiglas channel and its velocity was varied in the range of about 3~9cm/s. Uniformity of vertical velocity was checked by traversing a magnetic velocimeter at five different cross sections. Experimental set-up used for the case of flowing ambient water is shown in Fig.1. Experimental condition is tabulated in Table 1, where the particle with median diameter d=0.044mm is glass bead and the others are sieved sediments, and the values of W_0 and A_0 are the half of total initial buoyancy and volume per unit width.

Velocity and shape of the particle cloud along its pass were quantified by a flow visualization technique; a VTR-camera was moved along pre-determined trajectory of the cloud that visualized

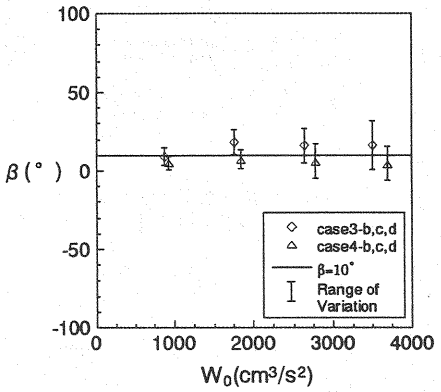

Fig.4 Dependence of inclination angle β with respect the main axis on W_0

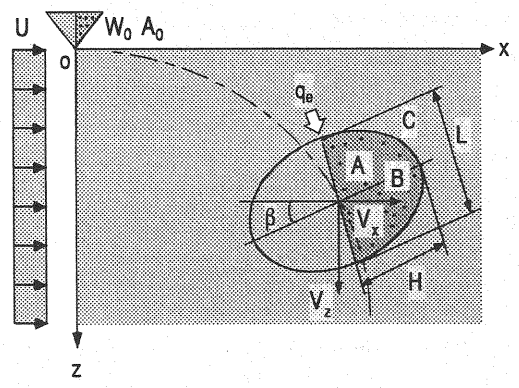

Fig.5 Schematic of the falling cloud in ambient water

by laser slit beam. Analysis of the image of clouds recorded by the VTR, whose sampling interval can be controlled by a computer, allows to obtain the horizontal as well as falling velocity and the shape of the clouds. Repeatability of experiments was satisfactory, so that flow characteristics of the cloud were determined based on five set of experimental data repeated under the same condition.

Figs. 2a and 2b show the motion of the particle clouds falling in quiescent ambient water (CASE2-a-3) and in flowing ambient water(CASE2-b-4), respectively. It may be observed that the shape of particle clouds is approximately symmetric with respect to the main axis of the clouds even in the case that ambient water is flowing, and the cloud in flowing water falls and at the same time advects horizontally, actively entraining fresh water. Similar to the cloud falling in quiescent water(Fig. 2a), the cloud has approximately an elliptical shape, and geometrical similarity of the cloud is maintained along its path. Such characteristics are demonstrated in Fig. 3, where the major and minor axis are normalized by maximum length in each direction. It is different from the case of quiescent water that the cloud falls with the inclination angle β with respect to the main axis of the cloud, and the magnitude of β is dependent neither on the amount of W_o nor U although β-values fluctuate in falling process as shown in Fig. 4. Based on this observation, the motion of the cloud falling in flowing water is modeled as schematically depicted in Fig. 5, where L is the length, H the half-width , C the half-circumference, q_e the rate of entrained ambient water, V_z the falling velocity, V_x the horizontal speed, A the half-area and B the average half-buoyancy of the cloud. Naturally, both β and V_x are zero for the cloud falling in quiescent water, i.e., U=0.

EXPERIMENTAL RESULTS

Prior to examining flow characteristics of the particle clouds, the flow regime of the motion of the clouds dealt in this study is identified.

According to the thermal theory(3), such major flow characteristics as H, B and V_z of a fully developed homogeneous dense cloud falling through quiescent ambient water are given respectively as

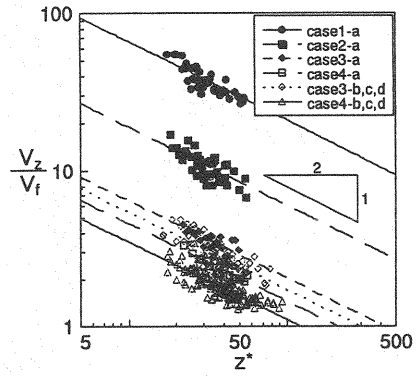

Fig.6 Relationship between dimensionless falling speed of the cloud V_z/V_f and dimensionless falling distance z^*

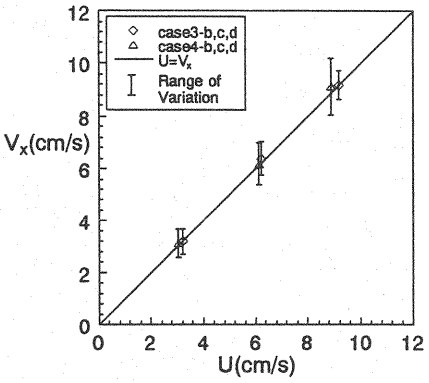

Fig.8 Relationship between the horizontal velocity V_x and the ambient flow velocity U

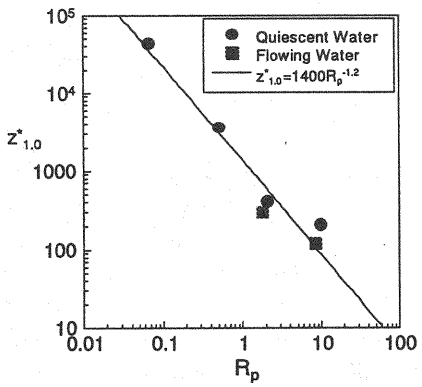

Fig.7 Transitional condition between the thermal -like phase and the free settling-like phase

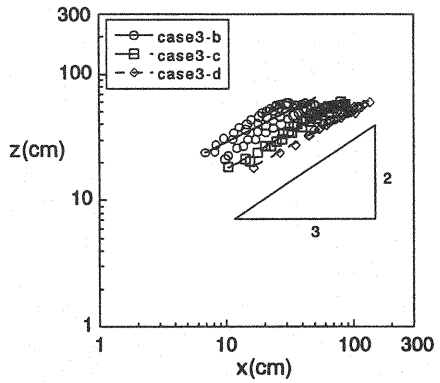

Fig.9 Example of trajectory of the particle cloud in flowing water

$$\frac{H^*}{z^*} = K_1 \qquad (1)$$

$$\frac{B^*}{z^{*-2}} = K_2 \qquad (2)$$

$$\frac{V_z^*}{z^{*-1/2}} = K_3 \qquad (3)$$

The independent variable in the preceding equations has to be a falling distance measured from a virtual origin $\tilde{z}$ instead of a falling distance measured from water surface z. However, for a fully developed thermal the solutions expressed by $\tilde{z}$ are identical to those by z, and hence they are expressed in terms of z. Because such expression is physically more meaningful. The dimensionless maximum half-width H^*, dimensionless average buoyancy B^*, dimensionless falling

velocity V_z^* of the clouds and the dimensionless falling distance z^* are defined respectively as $H^*=H/z_0$, $B^*=B/B_0$, $V_z^*=V_z/V_0$ and $z^*=z/z_0$, in which z_0, B_0 and V_0 are the representative length, buoyancy force and velocity scale based on the initial conditions, respectively. These representative scales are introduced to exclude the effects of the initial conditions.

$$z_0 = A_0^{1/2} \tag{4}$$

$$B_0 = \frac{W_0}{A_0} \tag{5}$$

$$V_0 = (sgW_0)^{1/4} \tag{6}$$

K_1, K_2 and K_3 in Eqs(1), (2) and (3) are given respectively by

$$K_1 = \frac{1}{2}\left(\frac{S_2}{S_1}\right)\sqrt{F}E_d \tag{7}$$

$$K_2 = \frac{\frac{F}{S_1}}{\left\{\frac{1}{2}\left(\frac{S_2}{S_1}\right)\sqrt{F}E_d\right\}^2} \tag{8}$$

$$K_3 = \sqrt{\frac{2\alpha_2}{(\alpha_1 - 1)}} \tag{9}$$

α_1 and α_2 in Eq.9 are parameters given respectively by

$$\alpha_1 = 4\left\{1 + \frac{\sqrt{F}c_d}{(1+A_m)E_d^2 S_2^2}\right\} \tag{10}$$

$$\alpha_2 = \frac{4 S_1 W_0}{(1+A_m)E_d^2 S_2^2} \tag{11}$$

where F is the length-to-height ratio of the cloud

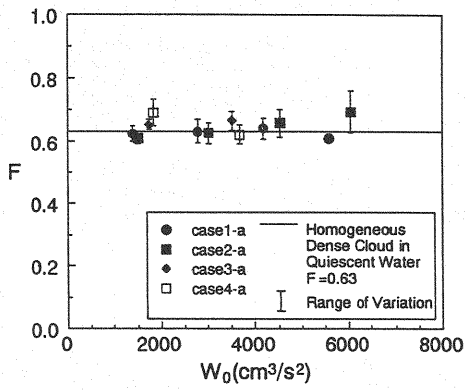

(a)

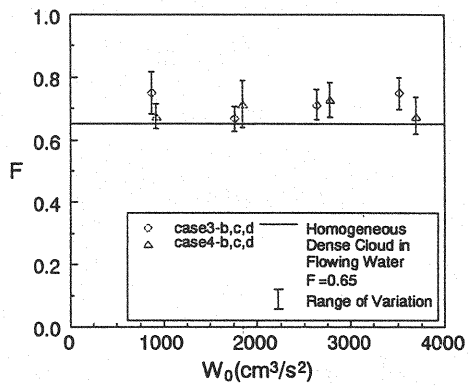

(b)

Fig.10 Dependence of the length-to-height ratio F on initial total buoyancy W_0 (a:quiescent ambient water, b:flowing ambient water)

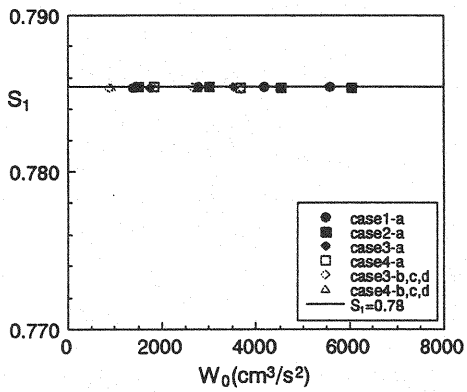

Fig.11 Dependence of the volume correction factor S_1 on initial total buoyancy W_0

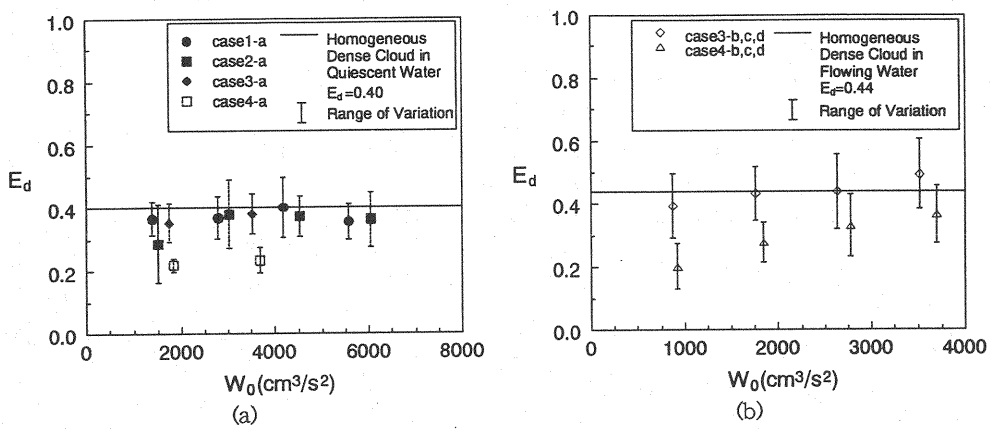

Fig.12 Relationship between the entrainment coefficient E_d and W_0
(a;quiescent ambient water, b:flowing ambient water)

($=H/L$), E_d the entrainment coefficient($=q_e/CV_z$), C_d the drag coefficient,and A_m the added mass coefficient($=2F$). q_e is the amount of entrained ambient fluid per unit time, and C is the half-circumference of the cloud. S_1 and S_2 are shape factors defined respectively by

$$S_1 = \frac{A}{HL} \tag{12}$$

$$S_2 = \frac{C}{\sqrt{HL}} \tag{13}$$

For an elliptical shape, these shape factors are given respectively by

$$S_1 = \frac{\pi}{4} \tag{14}$$

$$S_2 = \frac{\left(\pi / 2^{3/2}\right)\sqrt{4F^2+1}}{\sqrt{F}} \tag{15}$$

In case of the homogeneous dense cloud, initial total buoyancy per unit width W_0 is defined as $W_0=\varepsilon_0 g A_0'$, where A_0' is the initial volume of dense fluid per unit width. The initial relative density difference of the cloud ε_0 is defined as $\varepsilon_0=((\rho_0-\rho_a)/\rho_a)$, in which ρ_0 is the initial density of dense fluid. For the particle cloud, the initial density of water-particles mixture expressed in terms of volumetric concentration($c=0\sim1$) is given by $\rho_0=c_0\rho_p + (1-c_0)\rho_a$. Consequently, W_0 for the particle cloud can be expressed as $W_0=c_0 s g A_0'$ or $s g A_0$.

These theoretical result suggest that the motion of a fully developed homogeneous turbulent thermal is characterized as $H \propto z$, $B \propto z^{-2}$ and $V_z \propto z^{-1/2}$. It is known from our previous study(3) that among these major flow characteristics V_z is the most sensitive to the initial conditions(A_0', W_0). In Fig. 6, V_z of the particle clouds are plotted against z in dimensionless form; V_z is normalized

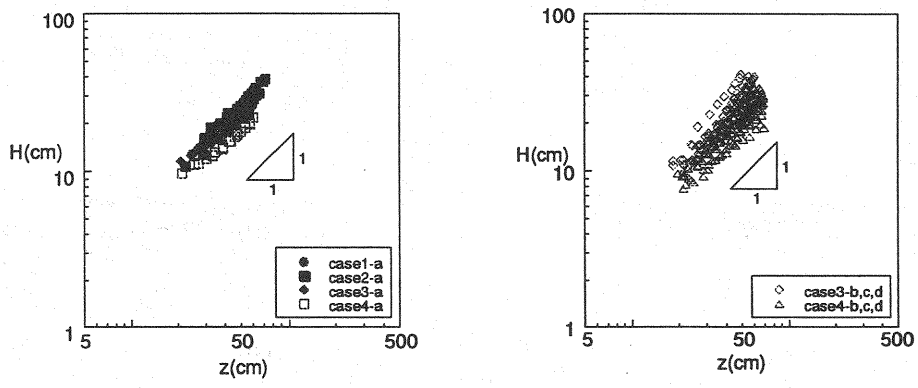

Fig.13 Dependence of maximum half-width H on falling distance z
(a:quiescent ambient water, b:flowing ambient water)

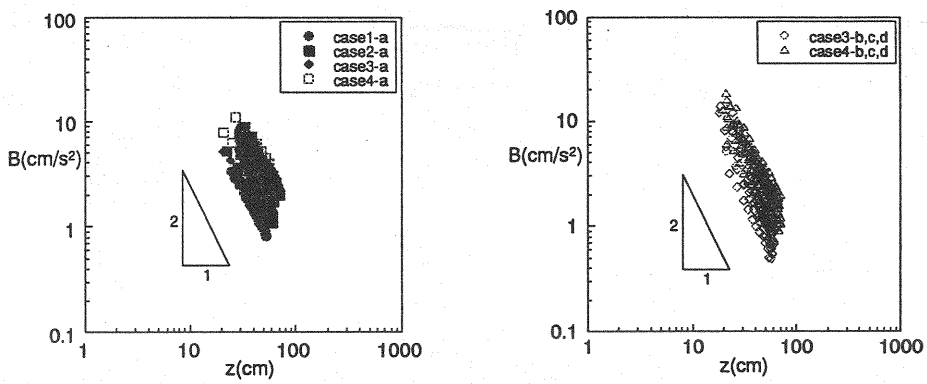

Fig.14 Dependence of average buoyancy B on flowing distance z
(a:quiescent ambient water, b:flowing ambient water)

by V_f in order to relate the falling speed of the cloud to the terminal settling velocity of particle. z is normalized by the representative length scale $A_o^{1/2}$ based on the initial conditions. As obvious from Eqs. 1,2 and 3, W_o is a controlling factor of the phenomena. For the particle cloud, W_o is given by sgA_o, but s is about constant. Hence, A_o is considered to represent the initial conditions.

Fig.6 shows that all date lie in the range of $V_z/V_f \geqq 1.0$ and follow the relationship of $V_z \propto z^{-1/2}$ This indicates that the motion of the particle clouds dealt in this study belongs to the thermal-like phase. As will be shown later, dependence of H and B on z are also confirmed to follow $H \propto z$ and $B \propto z^{-2}$, respectively. Similar to the homogeneous turbulent thermal, it can be identified from Fig. 6 that dependence of V_z/V_f on z^* is not affected by A_o or W_o, but is influenced by d and U. Fig. 6 also shows that the falling velocity of the cloud consisting of particles with median diameter can be often much larger than the terminal settling velocity of individual particles with the same diameter.

The falling distance that the particle cloud changes its motion from the thermal-like phase to

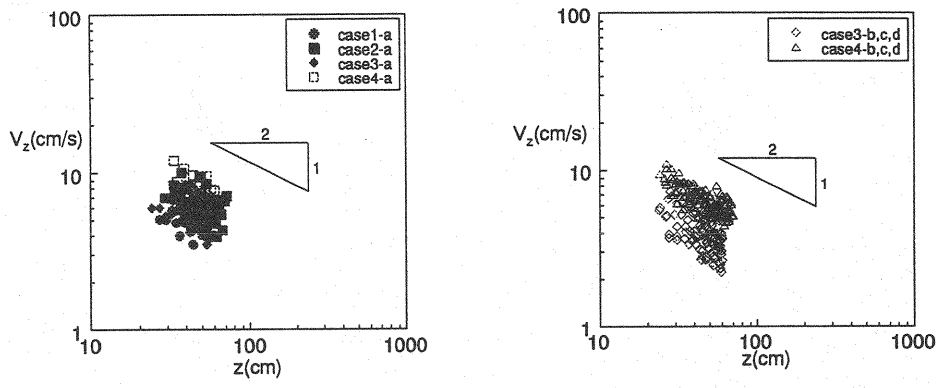

Fig.15 Dependence of falling velocity V_z on flowing distance z
(a:quiescent ambient water, b:flowing ambient water)

the free settling-like phase can be roughly estimated from Fig. 6. Fig. 7 shows dependence of $z^*_{1.0}$ on the particle Reynolds number $R_p(=dV_f/\nu)$, where $z^*_{1.0}$ is the value of z^* at V_z/V_f=1.0 in Fig. 6. Ignoring minor differences in the values of $z^*_{1.0}$ between the case of quiescent and flowing ambient water observed in Fig. 7, the transitional condition is roughly estimated as follow,

$$z^*_{1.0} = 1400 R_p^{-1.2} \qquad (16)$$

According to Tamai et al.(1), the motion of the particle cloud tends to take the thermal-like form when A_0 is large and d is small, whereas it to take the free settling-like form when A_0 is small and d is large. The falling velocity of the homogeneous turbulent thermal decreases rapidly as indicated by the relationship $V_z \propto z^{-1/2}$, so that turbulent intensity within the thermal body decreases accordingly with z. As a result, the motion of the particle cloud is expected to be changing from the thermal-like phase to the free settling-like phase. There is no investigation on the relationship between turbulent intensity within the cloud and the form of the cloud, but Eq.16 supports this consideration; Eq.16 suggests that the particle cloud is able to maintain the thermal-like motion in longer distance when A_0 is larger or d is smaller if ν is constant. Thus, it may be concluded that Tamai et al.'s finding is only true when, roughly speaking, ambient water depth is less than the falling distance given in Eq.16.

In the following sections, flow characteristics of the particle cloud in the thermal-like phase are examined.

Horizontal Velocity V_x and Trajectory of Particle Cloud

Fig. 8 shows the relationship between the horizontal speed of the particle cloud V_x and the ambient flow velocity U. It is seen that V_x fluctuates, but the average values of V_x are nearly equal to U. This means that the cloud falling in flowing water advects in the downstream direction at about the same speed as U. A similar finding, based on numerical simulation, have been

reported by Oda et al.(10).

Some examples of trajectory of the cloud in Fig. 9 indicate that z is proportional to $x^{2/3}$ even when the magnitude of U is different. This may be reasoned that V_z is proportional to $z^{-1/2}$, and hence z is proportional to $t^{2/3}$. On the other hand, the horizontal velocity V_x is constant, and hence x is proportional to t. By relating z with x through t, $z \propto x^{2/3}$ is obtained. This again confirms that the cloud in flowing water falls in a manner similar to those in quiescent water, and at the same time the cloud advects at about the same velocity as the ambient water velocity.

Length-to-Height Ratio F and Volume Correction Factor S_I

Dependence of the length-to-height ratio F and the volume correction factor S_I on W_0 are examined in Figs. 10 and 11, respectively. Results of the homogeneous cloud are also presented in these figures. Both F and S_I do not depend on W_0 even when the ambient water is flowing. In quiescent water, no significant difference in F-values between the homogeneous cloud and the particle cloud can be identified. But, in quiescent water F-values of the particle clouds in flowing water are larger than those of the homogeneous cloud. F-values for the particle cloud in quiescent water is approximated as 0.63 and those in flowing water as 0.70. While, S_I-values of the particle cloud are identical to those of the homogeneous cloud in quiescent water and are approximated as 0.785. This is the S_I-value for an ellipse, that is, $\pi/4$.

Entrainment Coefficient E_d

Fig. 12 shows relationship between the entrainment coefficient E_d and W_0. It may be observed from Fig. 12a that in the quiescent water E_d-values are not dependent on W_0, but on particle size d. For the clouds consisting of small particles E_d-values are almost equal to those of the homogeneous dense cloud,but for the cloudof larger particles E_d-values are smaller than those. It may be observed from Fig. 12b that in flowing water E_d-values are not only dependent on d, but also on W_0.

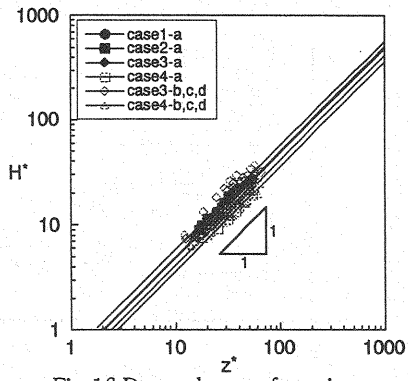

Fig.16 Dependence of maximum half-width H^* on falling distance z^*

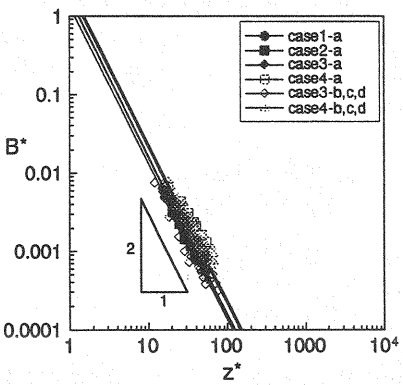

Fig.17 Dependence of average buoyancy B^* on falling distance z^*

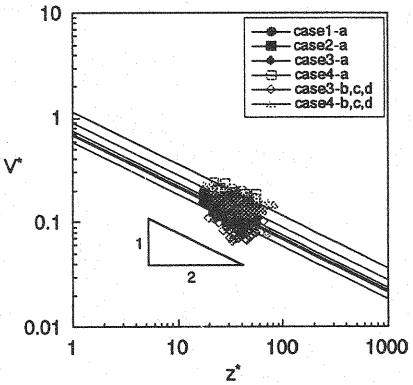

Fig.18 Dependence of falling velocity V^* on falling distance z^*

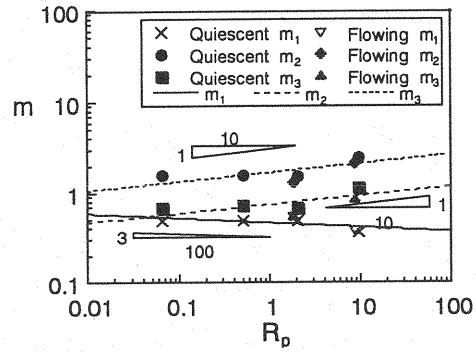

Fig.19 Dependence of m_l on R_p

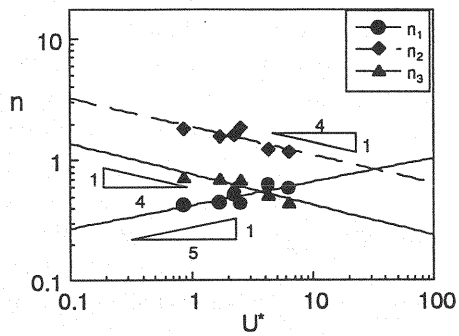

Fig.20 Dependence of n_l on U^*

E_d-values increase with W_0, and become smaller when the size of particles increase. The reason why W_0 affects the entrainment characteristics may be explained that the clouds with larger W_0 are less influenced by the presence of ambient flow, because of stronger circulating motion within the cloud.

Dimensionless Maximum Half-Width H^*, Dimensionless Average Buoyancy B^* and Dimensionless Falling Velocity V_z^*

Figs. 13, 14 and 15, respectively, show that dependence of the maximum half-width H, half-average buoyancy B and falling velocity V_z on the falling distance z. These figures clearly demonstrate that even in the case of flowing water such relationships as $H \propto z$, $B \propto z^{-2}$ and $V_z \propto z^{-1/2}$ are held. As far as the relationships between H, B, V_z and z are concerned, the motion of the particle cloud in the thermal-like phase can be also described by the thermal theory. However, it may be identified that the absolute values of these major flow characteristics are different, depending on the initial conditions(W_0, A_0), particle size d and ambient flow velocity U.

In what follows, we examine the effects of the initial conditions, particle diameter and ambient flow velocity on these major flow characteristics. Figs. 16, 17 and 18 show that the particle clouds follow the relationships of $H^* \propto z^*$, $B^* \propto z^{*-2}$ and $V_z^* \propto z^{*-1/2}$ in a manner similar to the homogeneous dense cloud, irrespective of the condition of ambient flow. The relationships are held even in the case of flowing water. Since the effects of the initial conditions on the motion of the clouds are excluded in these figures, comparisons between Figs. 13~15 and Figs. 16~18 reveal that the effects of the initial conditions on the motion are of particular significance. Furthermore, dependence of the major flow characteristics on z makes such an assumption possible that H^*, B^* and V_z^* of the particle cloud can be expressed in the following relations.

$$\frac{H^*}{z^*} = K_1' \tag{17}$$

$$\frac{B^*}{z^{*-2}} = K_2' \tag{18}$$

$$\frac{V^*}{z^{*-1/2}} = K_3' \qquad (19)$$

Herein, K_i' are coefficients to be determined, which may be different from K_i given in Eqs.4, 5 and 6. It is obvious from Figs. 16,17 and 18 that K_i' are affected by both d and U. Hence, we further assume that K_i' are expressed by the product of m_i the power of the particle Reynolds number R_p and n_i the power of the dimensionless ambient flow velocity $U^*(=U/V_f)$ as follows:

$$K_1' = R_p^{m_1} \cdot U^{*n_1} \qquad (20)$$

$$K_2' = R_p^{m_2} \cdot U^{*n_2} \qquad (21)$$

$$K_3' = R_p^{m_3} \cdot U^{*n_3} \qquad (22)$$

By utilizing the present experimental data,the values of exponent m_i and n_i are determined by the similarity collapse method(12). It is obvious that n_i are zero for the case of quiescent water. Figs. 19 and 20 shows how m_i and n_i are dependent on R_p and U^*, respectively. It may be realized from these figures that the values of m_i and n_i are different, depending on the flow characteristics and are well approximated as $m_1 \fallingdotseq 0.03$, $m_2 = m_3 \fallingdotseq -0.1$ and $n_1 \fallingdotseq 0.2$, $n_2 = n_3 \fallingdotseq -0.25$. Final results for these flow characteristics of the particle clouds falling through quiescent water are presented in Figs. 21, 22 and 23,respectively. It may be identified that the dimensionless parameter $H^* \cdot R_p^{0.03}$, $B^* \cdot R_p^{-0.1}$ and $V^* \cdot R_p^{-0.1}$ describe the motion of the particle clouds quite well. The same plots for the case of flowing water are presented in Figs. 24, 25 and 26.These figures show that $H^* \cdot R_p^{0.03}$, $B^* \cdot R_p^{-0.1}$ and $V^* \cdot R_p^{-0.1}$ are systematically dependent on the magnitude of U^* as presented in Fig. 20. Figs. 27, 28 and 29 are the results for flowing water. In this case, the

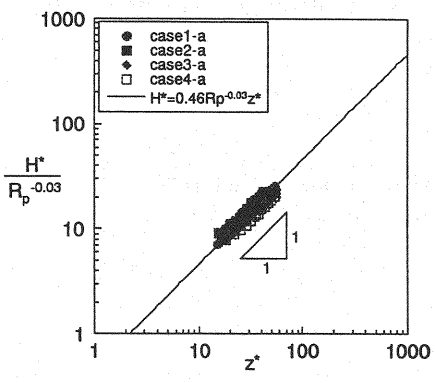

Fig.21 Relationship between $H^* \cdot R_p^{0.03}$ and falling distance z^*

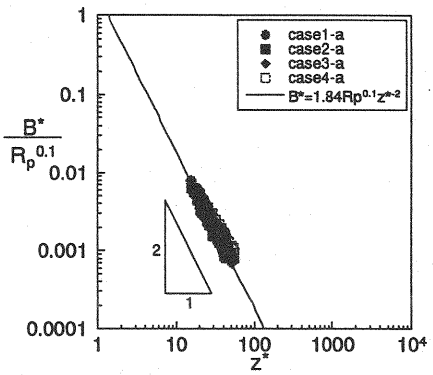

Fig.22 Relationship between $B^* \cdot R_p^{-0.1}$ and falling distance z^*

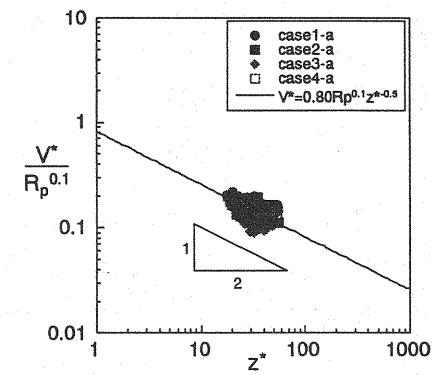

Fig.23 Relationship between $V^* \cdot R_p^{-0.1}$ and falling distance z^*

dimensionless parameter $H^* \cdot R_p^{0.03} \cdot U^{*-0.2}$, $B^* \cdot R_p^{-0.1} \cdot U^{*0.25}$ and $V^* \cdot R_p^{-0.1} \cdot U^{*0.25}$ can describe the motion of the particle cloud adequately. In summary, H^*, B^* and V_z^* for the range of $R_p \fallingdotseq 0.065 \sim 9.60$ and $U^* \fallingdotseq 0.85 \sim 6.21$ can approximately be expressed by the following empirical relationships.

For quiescent ambient water:

$$H^* = 0.46 R_p^{-0.03} z^* \quad (23)$$

$$B^* = 1.84 R_p^{0.1} z^{*-2} \quad (24)$$

$$V^* = 0.80 R_p^{0.1} z^{*-1/2} \quad (25)$$

For flowing ambient water:

$$H^* = 0.42 R_p^{-0.03} U^{*0.2} z^* \quad (26)$$

$$B^* = 1.86 R_p^{0.1} U^{*-0.25} z^{*-2} \quad (27)$$

$$V^* = 0.76 R_p^{0.1} U^{*-0.25} z^{*-1/2} \quad (28)$$

As far as the motion of the cloud remains in the thermal-like phase, such major flow characteristics of the particle cloud as H, B and V_z are affected by the initial conditions and the particle size,and the ambient flow velocity for the case of flowing ambient water. These major flow characteristics are mainly controlled by the initial conditions in a manner similar to the homogeneous dense cloud. The motion of the particle cloud is somewhat influenced by the size of particles.Larger particle contributes to increase of the falling velocity V_z and reduction of the half -width H of the cloud. The reason why the average buoyancy force B is also affected by particle size may be explained by the experimental evidence that the entrainment

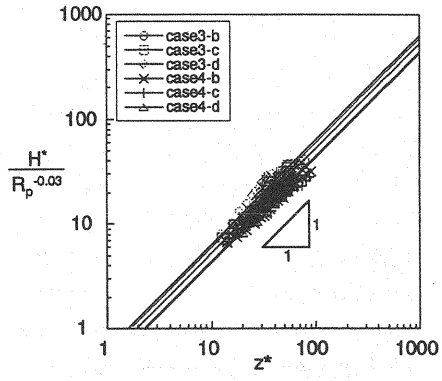

Fig.24 Relationship between $H^* \cdot R_p^{0.03}$ and falling distance z^*

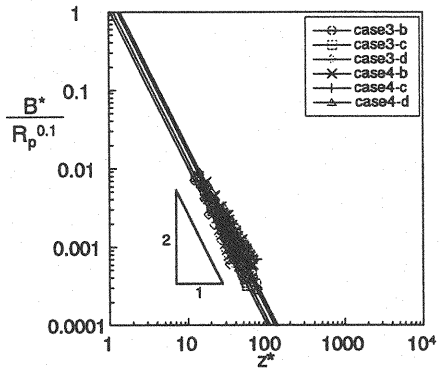

Fig.25 Relationship between $B^* \cdot R_p^{-0.1}$ and falling distance z^*

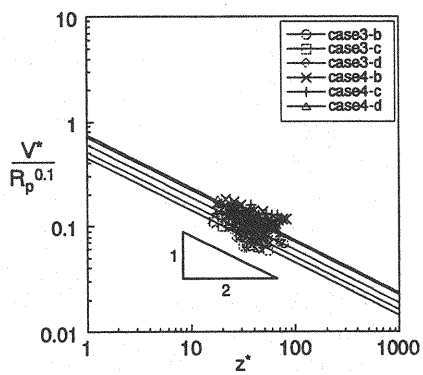

Fig.26 Relationship between $V^* \cdot R_p^{-0.1}$ and falling distance z^*

characteristic is affected by the size of particles. The presence of ambient flow is an additional factor to control the motion of the cloud. When ambient water velocity is smaller than a certain magnitude, the shape of the cloud is maintained along its pass as seen in Figs.2 and3. However, a pair of recirculating motion, that characterizes the motion of cloud,becomes less definite, and hence the major flow characteristics may be altered from those in quiescent water. This explanation is well supported by the results of previous numerical simulation(10).

CONCLUSIONS

Although the range of values of the parameters in the experimental conditions is limited, several important findings can be obtained from this study: (1)The falling distance of the particle cloud, that changes its motion from the thermal-like phase to the free settling-like phase, depends on the dumped volume and size of particles. The thermal-like motion can be maintained longer when the amount of dumped particles is larger and/or the particle size is smaller. (2) As far as the particle cloud is in the thermal-like phase, dependence of such major flow characteristics of the cloud as H, B and V_z on the falling distance follow the relationships of the homogeneous turbulent thermal theory, namely, $H \propto z$, $B \propto z^{-2}$ and $V_z \propto z^{-1/2}$, irrespective of the condition of ambient flow. The proportional constants K_i' are different from those of the homogeneous dense cloud, i.e., K_i. (3) The major flow characteristics of the particle cloud are affected by the size of particles, an those effects on the motion of the cloud are described by the particle Reynolds number R_p. The effects of R_p on H, B and V_z are somewhat different. H is the least sensitive to R_p, and decreases as R_p increases. B and V_z are equally sensitive to R_p, and both increase with R_p. (4) For the case of the flowing ambient water, the particle cloud advects at about the same velocity as the ambient flow velocity. H, B and V_z of the

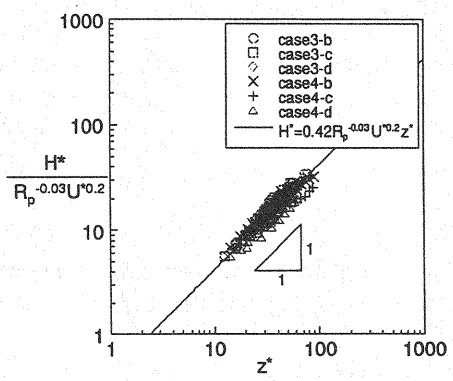

Fig.27 Relationship between $H^* \cdot R_p^{0.03} \cdot U^{*-0.20}$ and falling distance z^*

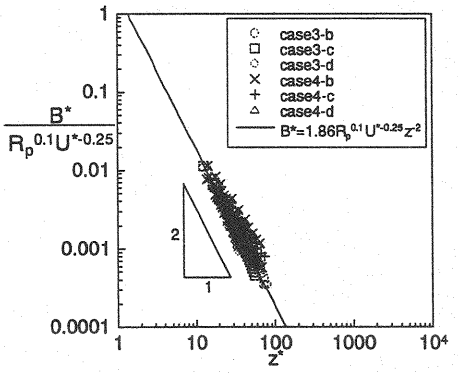

Fig.28 Relationship between $B^* \cdot R_p^{-0.1} \cdot U^{*0.25}$ and falling distance z^*

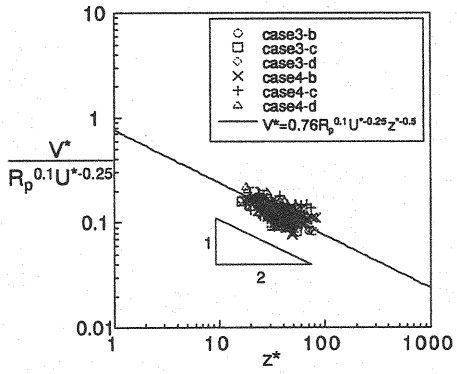

Fig.29 Relationship between $V^* \cdot R_p^{-0.1} \cdot U^{*0.25}$ and falling distance z^*

particle cloud are influenced by the magnitude of ambient flow, and those effects on the motion of the cloud are described by the dimensionless ambient water velocity U^*. H is the least sensitive to U^*. B and V_z are almost equally sensitive to U^*. H increases with U^*, but B and V_z decrease with U^*.

ACKNOWLEDGMENTS

This research was supported by the Grant-in-Aid for Science Research for Ministry of Education and Culture,Japan under Grant B(2), No.08455232 and No.12555149.

REFERENCES

1. Tamai, M., K. Muraoka and A. Murota:Study on falling behaviour of a swarm of solid particles and induced flow field , J. of Hydraulic, Coastal and Environmental Engineering, JSCE, No.509/Ⅱ -30, pp.143-154, 1995(in Japanese).
2. Baines, W. D and E. J. Hopfinger : Thermals with large density difference, Atomospheric Environment, Vol. 18, No. 6, pp.1051-1057, 1984.
3.Akiyama,J. ,M.Ura ,X.Ying, M. Imamiya and M.Suyama:Flow characteristics of dense cloud instantaneously released into quiescent fluid, Ann. J. of Hydraulic Engineering, Vol.42, pp.529-534、1998(in Japanese).
4.Buhler, J. and D.A. Papantoniou : Swarms of coarse particles falling through a fluid, Proc. of the Int'l Symposium on Environmental Hydraulics, Vol.1, pp.135-140, 1991.
5.Horie, T.:MAC model for prediction of short-term fate of dumped material from barge, Technical Note of port & Harbour Research Institute, No.471, pp.1-34, 1983(in Japanese).
6.Oda,K., T. Shigematsu, N. Onishi and M. Inoue:Numerical simulation of settling and spreading behavior of particle cloud using improved DEMAC method, Proc. of coastal Engineering, JSCE, Vol.39, pp.971-975, 1992(in Japanese).
7.Li, C.W.:Convection of particle thermals, J. Hydraulic Research, Vol.35, No.3, pp.363-376, 1997.
8.Ying.X., J.Akiyama and M.Ura : Motion of dense fluid released into quiescent water with finite depth, J. of Hydraulic, Coastal and Environmental Engineering, JSCE, No.635/Ⅱ-49, pp.141-152, 1999.
9.Cundall, P.A. : Rational design of tunnel supports, Technical Report MRD-2-74, U.S. Army Corps of Engineers, 1974.
10.Oda, K., ,T. Shigematsu and H.Kanno : Numerical experiments on the effects of ambient flow to the settling and dispersion of a mass of falling particles, Proc. of Coastal Engineering, JSCE, Vol.42, pp.1271-1275(in Japanese).
11. Akiyama,J., M.Ura, X.Ying, M. Imamiya and H.Nishimori : Experimental investigation on motion of dense cloud in uniform ambient flow,Ann. J. of Hydraulic Engineering, Vol.42、pp.1165-1170, 1998(in Japanese).
12.Akiyama,J. and Y. Fukushima : Entrainment of noncohesive bed sediment into suspension, Proc.3rd Int. Sym. River Sedimentation, Mississippi, USA, pp.804-813,1986.

APPENDIX-NOTATION

The following symbols are used in this paper:

A=volume of a cloud per unit width;
A_o=initial volume of particles par unit width;
A_o'=initial volume of dense fluid or water-particles mixture per unit width;
B=average buoyancy of a cloud;
$B^*=B/(W_o/A_o)$;
C=half-circumference of a cloud;
c=volumetric concentration(=0~1.0);
C_d=drag coefficient;
g=acceleration of gravity;
d=median diameter of a particle;
E_d=entrainment coefficient;
H=half-width of a cloud;
$H^*=h/A_o^{1/2}$;
K_i=proportional constants for a homogeneous dense cloud(i=1,2,3);
K_i'=proportional constants for a particle cloud(i=1,2,3);
L=length of a cloud;
R_p=particle Reynolds number;
S_1, S_2=shape factors;
s=submerged specific gravity of a particle;
t=time;
U=ambient flow velocity;
$U^*=U/V_f$;
V_f=free settling velocity of a particle;
V_o=representative falling velocity of a cloud based on initial conditions;
V_x=horizontal velocity of a cloud;
V_z=falling velocity of a cloud;
$V_z^*=V_z/(sgW_o)^{1/4}$;
W_o=initial total buoyancy;
x=horizontal coordinate;
z=vertical coordinate;
z_o=representative length scale based on initial conditions;
ρ_a=density of ambient water;
ρ_o=initial density of homogeneous dense fluid or water-particles mixture;
ρ_p=density of particle;
ε_o=initial relative density difference of homogeneous dense fluid or water- particles mixture; and
σ=specific gravity of particle.

(Received December 9, 1999 ; revised April 8, 2000)